

Auger effect in high-resolution Ce 3*d*-edge resonant photoemission

E.-J. Cho

Department of Physics, Chonnam National University, Kwangju 500-757, Korea

R.-J. Jung, B.-H. Choi, and S.-J. Oh

School of Physics and Center for Strongly Correlated Materials Research, Seoul National University, Seoul 151-742, Korea

T. Iwasaki, A. Sekiyama, S. Imada, and S. Suga

Department of Material Physics, Graduate School of Engineering Science, Osaka University, Toyonaka, Osaka 560-8531, Japan

T. Muro

Japan Synchrotron Radiation Research Institute, Sayogun, Hyogo 679-5198, Japan

J.-G. Park, and Y. S. Kwon

Department of Physics, Sung Kyun Kwan University, Suwon 440-746, Korea

(Received 1 October 2002; published 15 April 2003)

The bulk-sensitive Ce 4*f* spectral weights of various Ce compounds including CeFe₂, CeNi₂, and CeSi₂ were obtained with the resonant photoemission technique at the Ce 3*d* edge. We found that the line shapes change significantly with the small change of the incident photon energy. Detailed analysis showed that this phenomenon results primarily from the Auger transition between different multiplet states of the Ce $\overline{3d_{5/2}}4f^2$ (bar denotes a hole) electronic configuration in the intermediate state of the resonant process. This tells us that extra care should be taken for the choice of the resonant photon energy when extracting Ce 4*f* spectral weights from the Ce 3*d*-edge resonant photoemission spectra. The absorption energy corresponding to the lowest multiplet structure of the Ce $\overline{3d_{5/2}}4f^2$ configuration seems to be the logical choice to obtain genuine Ce 4*f* spectral weight from the Ce 3*d* resonant photoemission data.

DOI: 10.1103/PhysRevB.67.155107

PACS number(s): 71.28.+d, 73.20.At, 79.60.-i

I. INTRODUCTION

Investigations on the electronic structures of strongly correlated materials such as *d* and *f* electron systems have been very active lately.^{1,2} One of the perhaps oldest problems in this category is the origin of the $\alpha \rightleftharpoons \gamma$ phase transition of Ce metal and its compounds, which has been studied for more than 50 years but still remains controversial.³⁻⁵ Photoemission spectroscopy, among various experimental techniques, is a very powerful tool that can directly probe the electronic structures of solids. Indeed in the case of Ce problem as well, the study of 4*f* spectral weights of various Ce compounds using resonant photoelectron spectroscopy (RPES) technique at the Ce 4*d* edge contributed decisively to the understanding of this famous phase transition. This technique is necessary to enhance the 4*f* electron emissions and separate them from contributions of other conduction electrons,⁶ and utilizes the following process

$$4d^{10}4f^1 + \hbar\omega \rightarrow 4d^9 4f^2 \rightarrow 4d^{10}4f^0 + \text{photoelectron.} \quad (1)$$

The conventional wisdom that came out of these studies, at least until early 1990s, was as follows. The major factor distinguishing between α and γ phases of Ce and its compounds is the strength of the hybridization between Ce 4*f* level and the conduction bands, and the disappearance of the local magnetic moment in the α phase results from the Kondo phenomenon of the singlet formation due to the hybridization of a localized 4*f* electron with conduction elec-

trons, and not from the promotion of the 4*f* electron to the empty state above the Fermi level.³⁻⁵

After the high-resolution RPES was developed in the early 1990s, however, some groups questioned this conventional wisdom and proposed a new interpretation of the 4*f* spectral weights of Ce compounds.^{7,8} The main point of those groups was that the temperature or the material dependence of the 4*f* spectral weights of Ce compounds near the Fermi level, which had been interpreted as the tail of the Kondo resonance,⁹ did not follow the Kondo scenario which stipulates that the Kondo temperature is the universal controlling parameter that determines the strength of the Kondo resonance near the Fermi level in different materials or at different measuring temperatures. This controversy generated many more careful studies on the 4*f* spectral weights of various Ce compounds by several research groups,¹⁰⁻¹⁴ some utilizing RPES technique and others using ordinary ultraviolet photoemission (UPS) technique with He_I ($h\nu=21.2$ eV) and He_{II} ($h\nu=40.8$ eV) sources.

Most of these later studies also supported Kondo resonance scenario, but one important issue that has not been settled so far is the surface effect and how to separate the surface from the bulk contributions.¹⁵ Since the electron kinetic energy at the Ce 4*d*-edge RPES is about 120 eV, and the electron mean free path at this kinetic energy is only about 5 Å,^{16,17} the surface contribution in the 4*f* spectral weights obtained with 4*d*-edge RPES technique is expected to be very much significant, even larger than the bulk in some cases. The situation with the ordinary UPS data with

He_I ($h\nu=21.2$ eV) and He_{II} ($h\nu=40.8$ eV) sources is not much different. Hence to compare quantitatively the experimental photoemission spectra with those expected from the Kondo temperature of bulk materials, it is imperative to be able to extract the bulk contributions from the experimental data. Many approaches have been tried with the Ce $4d$ -edge RPES or ordinary UPS data,^{13,14} but the results were not conclusive enough since each method has its own drawbacks and uncertainties.

Recently a powerful new method to extract reliable bulk Ce $4f$ spectral weights has become possible thanks to the advent of the new beamline at SPring-8, Japan.¹⁸ It has been well known that we can reduce the surface contribution in photoemission spectra by using high energy photon source. For example, if around 880 eV photon source is used in RPES, the electron mean free path of the photoelectrons from Ce $4f$ levels will be about 20 Å.^{16,17} Since those 880-eV photon energies can excite a Ce $3d$ core electron to an empty $4f$ level (Ce $3d$ absorption edge), the $4f$ spectral weight is also enhanced due to the resonance phenomenon as in the case of Ce $4d$ -edge RPES. Hence we can obtain much more bulk-sensitive Ce $4f$ spectral weights by using those high photon energies in this so-called Ce $3d$ -edge RPES technique. In fact, this technique had been already tried more than 10 years ago,¹⁹ but the energy resolution in the Ce $3d$ -edge RPES at that time was not good enough to give conclusive results. Recently, Sekiyama *et al.* succeeded to obtain the total energy resolution including energy analyzer at the Ce $3d$ -edge photon source less than 100 meV with high photon flux in the undulator beamline of SPring-8 and study high-resolution bulk-sensitive Ce spectral weights in CeRu₂.²⁰ This opened up a new possibility to extract reliable bulk-sensitive spectral weights in many interesting Ce compounds, and several papers have already appeared utilizing this Ce $3d$ -edge RPES technique.²⁰⁻²²

However, in the course of this study, we realized that the experimental photoemission data depend sensitively on the exact incident photon energy near the Ce $3d$ edge, and the difference of spectral line shape is significant enough to affect data interpretation. Also the new Ce $3d$ -edge RPES data were found to be not completely consistent with the old data taken in early 1990s, even after the difference of the energy resolutions is taken into account. To derive reliable conclusions from the Ce $3d$ -edge RPES data, therefore, it is necessary to understand the origin of these differences and changes. This paper is an attempt to understand the origin of these phenomena by systematically studying Ce $3d$ -edge RPES of several Ce compounds. We will show in this paper data on CeFe₂, CeNi₂, and CeSi₂ only, although we studied many more Ce compounds which gave fully consistent results with the conclusion of this paper. The three Ce compounds to be discussed here have various Kondo temperatures, the universal parameter that controls many physical properties of Ce compounds in the Kondo resonance scenario. The Kondo temperatures of intermetallic compounds CeFe₂ and CeNi₂ are larger than about 500 K, and that of CeSi₂ compound is about 45 K.^{4,5} This paper will mainly focus on the general phenomena of the Ce $3d$ -edge RPES,

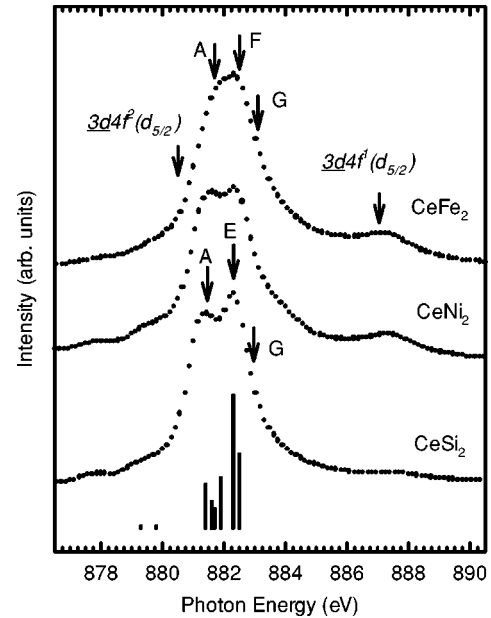


FIG. 1. x-ray absorption spectra of $3d \rightarrow 4f$ transition region for CeFe₂, CeNi₂, and CeSi₂. The symbols marked on the spectrum represent photon energies used for RPES shown in subsequent figures. The bar diagram at the bottom is the theoretical calculation result for the multiplet structure of $3df^2$ intermediate state taken from Ref. 26.

and the electronic structures of individual compounds will be discussed in separate publications.^{23,24}

II. EXPERIMENT

Polycrystalline samples of CeFe₂, CeNi₂, and CeSi₂ were made by the arc-melting method under Ar gas environment with constituent elements Ce, Fe, Ni, and Si whose purity was better than 99.9%. The homogeneity of samples was checked after annealing with x-ray diffraction.

Resonant photoemission spectra of the valence bands at various photon energies near the Ce $3d$ edge ($h\nu \sim 880$ eV) along with the Ce $3d$ -edge x-ray absorption spectrum (XAS) were obtained at the beamline BL25SU in the SPring-8 of Japan.¹⁸ The base pressure of an analysis chamber was about 3×10^{-10} mbar or better. The samples were scraped with a diamond file to get clean surfaces, and every time the cleanness of sample surface was checked with the O $1s$ core-level spectrum. If the oxygen contamination peak was found noticeable in O $1s$ core-level spectrum, the samples were scraped again with the diamond file. All spectra were measured at the temperature of 20 K, and the scraping was also done at 20 K. The XAS measurements were done by the total electron yield mode, and the energy resolution was about 80 meV. Scienta 200 analyzer was used for the electron energy analysis for PES measurements, and the total resolution of the PES spectra was better than 100 meV.

III. DATA AND DISCUSSIONS

Figure 1 shows the Ce M_V XAS data representing $3d_{5/2} \rightarrow 4f$ transition for CeFe₂, CeNi₂, and CeSi₂ compounds.

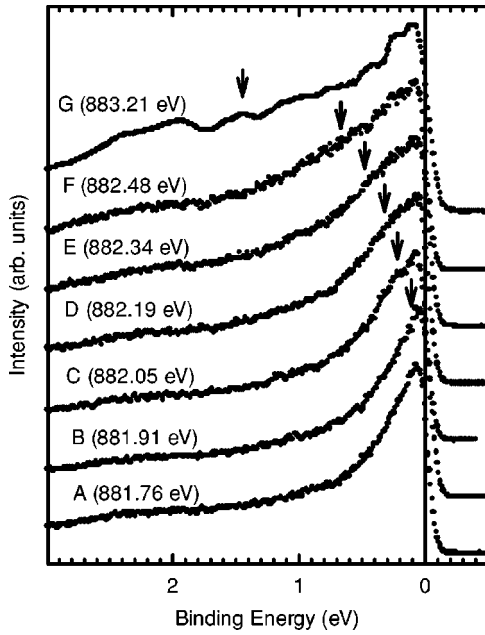


FIG. 2. Ce f spectral weights near the Fermi level for CeFe_2 obtained with various incident photon energies.

The $3d_{5/2}$ XAS of Fig. 1 consists of the main peak structure near $h\nu=882$ eV, and the satellite peak near $h\nu=887$ eV. The main peak structure comes from “ $3d^{10}4f^1$ ” \rightarrow “ $3d^94f^2$ ” transition, and the satellite peak “ $3d^{10}4f^0$ ” \rightarrow “ $3d^9f^1$ ” transition.²⁵ The quotation mark indicates approximate interpretation, since the complete eigenstate of each peak is composed of many body configurations. The line shape of the main peak near 882 eV is primarily determined by the multiplet structures of the $3d4f^2$ electronic configuration, where the underline represents a hole. At the bottom of the figure is shown the theoretical bar diagram, which represents energy positions and intensities of the multiplets of the $3d_{5/2}4f^2$ electronic configuration expected from the atomic calculation.²⁶ We can see that the theoretical calculation compares favorably with the experimental XAS data, especially for the case of CeSi_2 , although we can also notice that the details of the main peak line shape and the satellite peak intensity near 887 eV change somewhat depending on the compounds. This change of the XAS line shape is due to the stronger hybridization between Ce $4f$ electron and the conduction band in CeFe_2 and CeNi_2 compared with CeSi_2 , as evidenced by their Kondo temperatures. We will deal with this phenomenon and its implication on the electronic structures systematically in a separate publication.²⁴ In this figure, the symbols A to G designate the incident photon energies used to obtain the $4f$ spectral weights with the Ce $3d$ -edge RPES to be shown in subsequent figures.

Figure 2 represents RPES spectra near the Fermi level of CeFe_2 obtained with various incident photon energies corresponding to the symbols from A to G in Fig. 1. All through these photon energies the Ce $4f$ spectral weights are resonantly enhanced by the following process.

$$3d^{10}4f^1 + \hbar\omega \rightarrow 3d^94f^2 \rightarrow 3d^{10}4f^0 + \text{photoelectron}. \quad (2)$$

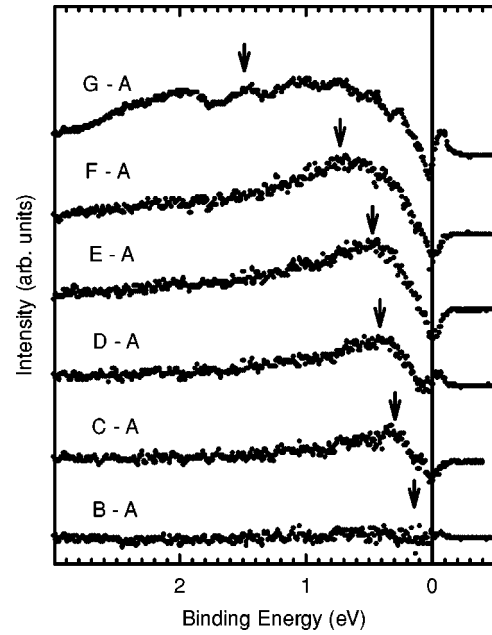


FIG. 3. Difference spectra between the $4f$ spectral weights at various photon energies and that at $h\nu=881.76$ eV.

Since the contribution from the Ce $4f$ emissions is at least ten times larger than those from other conduction electrons at these resonance energies, we can safely neglect the other conduction-electron contributions and consider the spectra of Fig. 2 as the Ce $4f$ spectral weights near the Fermi level, as in the case of Ce $4d$ -edge RPES.^{4,6} However, the bulk contribution of Ce $4f$ spectral weights of Fig. 2 is much larger than that of $4d$ edge RPES, since the electron mean free path at $3d \rightarrow 4f$ transition energies is much longer.^{16,17}

The spectra in Fig. 2 consist of a peak near the Fermi level and a shoulder at about 2 eV. The shoulder near 2eV comes from the $f^1 \rightarrow f^0$ transition, whereas the peak near the Fermi level comes from $f^1 \rightarrow f^1\bar{c}$ transition (\bar{c} means the hole in the conduction band) which corresponds to the tail of the Kondo resonance peak.^{4,5,7-12,19-22} The detailed analysis on those peaks and their relation to the electronic structures of CeFe_2 have been dealt with in other papers.^{21,22} Here we focus on the change of the $4f$ spectral line shapes depending on the incident photon energy. We clearly see that as the photon energy is increased from A (881.76 eV) to F (882.48 eV), which is only 0.72 eV apart, the width of the peak near the Fermi level is significantly broadened. To see these changes of spectral weights more quantitatively, we subtracted the spectrum at A from data taken at higher photon energies after normalizing each spectrum at its maximum intensity. The resulting difference spectra at various photon energies are shown in Fig. 3.

We find two noticeable features in every difference spectrum of Fig. 3—a broad peak below the Fermi level E_F and a sharp dip at E_F . The maximum of the broad peak moves to the high binding energy side as the incident photon energy is increased. In fact, we note that the binding energy of the maximum position is exactly the same as the difference of two incident energies, which is indicated by the arrows. This tells us that the kinetic energy of the broad peak remains the

same regardless of the incident photon energy, a telltale signature of Auger emission. Hence, we can conclude that this broad peak results from the Auger transition, and that the apparent change of the spectral line shapes depending on the incident photon energy is due to these Auger emissions overlapping the resonant $4f$ photoemissions. This Auger process must be the Coster-Kronig type between different multiplets of the $3d^9 4f^2$ configuration in the intermediate state of RPES.

To obtain genuine Ce $4f$ spectral weights from RPES data, therefore, it is necessary to avoid the contribution from these overlapping Auger emissions. The best way to achieve this is probably to take the spectrum at the incident photon energy corresponding to the lowest multiplet of the intermediate state. Indeed, we can see in the figure that the difference spectrum between B and A is nearly flat, implying that the spectral shape is nearly identical for data taken near the lowest multiplet. We have also confirmed that the spectra taken at incident photon energies slightly below A remain identical in line shapes as that of A . This fact gives us an important lesson in extracting bulk-sensitive Ce $4f$ spectral weights using the $3d$ -edge RPES technique—that is, it is dangerous to use the incident photon energy which simply gives maximum resonance effect (such as peak E in Fig. 1), since at that energy the spectra might be contaminated with overlapping Auger emissions. It is instead best to choose the incident photon energy as low as possible which still gives appreciable resonance effect. Some of the previous Ce $3d$ -edge RPES experiments may have been performed at the photon energy of maximum resonance, in which case the data have to be interpreted with caution. This interpretation on the origin of the line-shape change with the incident photon energy can also explain the dip structure near E_F shown in Fig. 3. Because of the Auger transition between multiplets, the intensity of the Kondo resonance peak near E_F will be reduced while some intensities move to higher binding energy side. Therefore if each spectrum is normalized to its maximum height before subtraction, as we did in our case, a dip will show up near the Fermi level with negative intensity in the difference spectra.

This phenomenon of overlapping Auger emissions in the Ce $3d$ -edge RPES spectra is not limited to the particular case of CeFe_2 . In Fig. 4 and Fig. 5 are shown the Ce $3d$ -edge RPES data for CeNi_2 and CeSi_2 , respectively, taken at various incident photon energies. Again, we see that they both show changes of spectral shapes depending on the photon energy, similar to the case of CeFe_2 . The two spectra of CeNi_2 in Fig. 4 are obtained with the incident photon energies of 882.34 eV (E) and 881.54 eV (A), which are very close to each other and roughly correspond to two maximum points of $3d_{5/2}$ XAS spectrum of CeNi_2 in Fig. 1. But these two $4f$ spectral weights have appreciably different shapes in that the spectrum at photon energy E shows a fairly strong peak around 0.8 eV binding energy, which becomes very weak or absent in the spectrum A . To understand the origin of this change of spectral shape, we again took the difference spectrum of the two and showed it at the bottom of Fig. 4. We can see in this difference spectrum a broad peak with its maximum around 0.8 eV binding energy, which is exactly

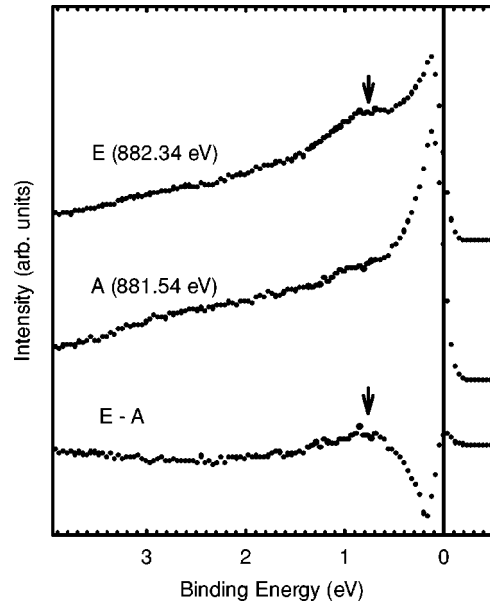


FIG. 4. Ce $4f$ spectral weights near the Fermi level for CeNi_2 obtained at different photon energies. Shown in the bottom is the difference spectrum between the two.

the difference of the photon energy and therefore corresponds to the constant kinetic energy feature. This tells us that in this case of CeNi_2 as well the origin of this phenomenon is the same as the case of CeFe_2 discussed earlier, and the overlapping Auger emissions between different multiplets of $3d^9 4f^2$ intermediate state contribute to the line-shape change with the incident photon energy. The CeSi_2 spectra shown in Fig. 5 give the same story, although the phenomenon does not look as pronounced as in the case of CeNi_2 . It is in fact a general observation in our series of Ce $3d$ -edge

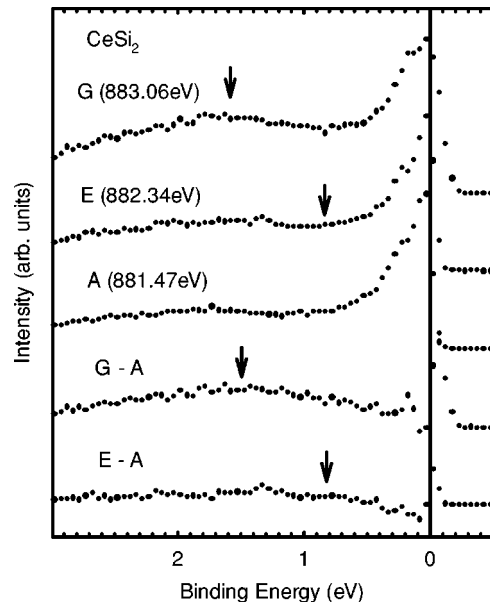


FIG. 5. Ce $4f$ spectral weight near the Fermi level for CeSi_2 obtained at various photon energies. In the bottom the difference spectra are shown.

resonant photoemission study on Ce compounds that the intensity of the indirect Auger emissions is weaker for a weakly hybridized system with a low Kondo temperature. This seems quite natural since the indirect Auger transition should involve a decay process into the delocalized conduction-band states, the probability of which must be higher when the hybridization between 4*f* and conduction-band electrons is strong and the density of conduction-band states near the Fermi level is large. Both of these trends will enhance the Kondo temperature of the material, hence explain the correlation between the indirect Auger emission intensity and the Kondo temperature.

We might mention that the observation of indirect Auger emissions in the valence-band spectrum obtained with incident photon energies higher than on-resonance in RPES is not unique to our cases discussed above. In fact, this phenomenon is quite common and much stronger in the metallic 3*d* and 4*d* systems, as observed, for example, in the Ni metal 3*p*-edge resonant photoemission.²⁷ The fact that this effect is rather small in Ce resonant photoemission compared to the cases of *d* electron systems is probably related to the more localized wave function of Ce 4*f* electron. Once the core hole is created by a photon in the x-ray absorption process, it can decay either to the direct Auger emissions without losing energy in the intermediate state, or to the indirect Auger emissions by losing some energy in the intermediate state by decaying into conduction-band states. The relative intensity of these two channels, i.e., direct Auger emissions versus indirect Auger emissions, will be determined by how fast the intermediate state decays into the conduction bands before the direct Auger emission takes place. Since this decay will be fast when the hybridization is strong between the localized state and the conduction band of the intermediate state, we can understand why the indirect Auger emissions are strong in transition-metal compounds compared with the more localized 4*f* compounds. The generally high

conduction-band density of states near the Fermi level for transition-metal compounds would also help this decay process, further enhancing indirect Auger emissions.

IV. CONCLUSION

In the newly developed Ce 3*d*-edge resonance photoemission technique for the study of bulk electronic structures of Ce compounds, the spectral shapes were found to depend sensitively on the incident photon energy. By analyzing Ce 3*d*-edge RPES valence-band spectra of CeFe₂, CeNi₂, and CeSi₂ compounds systematically, we showed that this phenomenon originated from the Auger transition between different multiplet structures of $3d4f^2$ electronic configuration in the intermediate state of the resonance process. Although we only showed the data on CeFe₂, CeNi₂, and CeSi₂ in this paper, we found similar results for other Ce compounds as well, and expect this phenomenon to be universal for any Ce compounds. Hence, when the Ce *f* spectral weights are obtained with the Ce 3*d*-edge RPES technique, it is very important to avoid these overlapping Auger emissions contributing to the spectra. The most logical choice of the incident photon energy to obtain genuine Ce 4*f* spectral weight from the Ce 3*d* resonant photoemission data must be that corresponding to the lowest multiplet of the 3*d*-edge x-ray absorption spectra.

ACKNOWLEDGMENTS

One of us (E.J.C.) acknowledges the support by Korea Research Foundation Grant (Grant No. KRF-2001-015-DP0178). This work was supported by the Korean Science and Engineering Foundation (KOSEF) through the Center for Strongly Correlated Materials Research (CSCMR) at Seoul National University. The research was performed under the support of Japan Synchrotron Radiation Research Institute (JASRI).

-
- ¹J.M. Lawrence, P.S. Riseborough, and R.D. Parks, Rep. Prog. Phys. **44**, 1 (1981).
²G.R. Stewart, Rev. Mod. Phys. **56**, 755 (1984).
³W.H. Zachariasen, Phys. Rev. **76**, 301 (1949); L. Pauling, J. Chem. Phys. **18**, 145 (1950).
⁴J.W. Allen, S.-J. Oh, O. Gunnarsson, K. Schonhammer, M.B. Maple, M.S. Torikachivili, and I. Lindau, Adv. Phys. **35**, 275 (1986).
⁵D. Malterre, M. Grioni, and Y. Baer, Adv. Phys. **45**, 299 (1996).
⁶J.W. Allen, S.-J. Oh, I. Lindau, J.M. Lawrence, L.I. Johansson, and S.B. Hagstrom, Phys. Rev. Lett. **46**, 1100 (1981).
⁷J.J. Joyce, A.J. Arko, J. Lawrence, P.C. Canfield, Z. Fisk, R.J. Bartlett, and J.D. Thompson, Phys. Rev. Lett. **68**, 236 (1992).
⁸R.I.R. Blyth, J.J. Joyce, A.J. Arko, P.C. Canfield, A.B. Andrews, Z. Fisk, J.D. Thompson, R.J. Bartlett, P. Riseborough, J. Tang, and J.M. Lawrence, Phys. Rev. B **48**, 9497 (1993).
⁹O. Gunnarsson and K. Schonhammer, Phys. Rev. Lett. **50**, 604 (1983); Phys. Rev. B **28**, 4315 (1983).
¹⁰D. Malterre, M. Grioni, P. Weibel, B. Dardel, and Y. Baer, Phys. Rev. Lett. **68**, 2656 (1992).
¹¹M. Grioni, P. Weibel, D. Malterre, Y. Baer, and L. Duo, Phys. Rev. B **55**, 2056 (1997).
¹²M. Garnier, K. Breuer, D. Purdie, M. Hengsberger, Y. Baer, and B. Delley, Phys. Rev. Lett. **78**, 4127 (1997).
¹³S.-H. Yang, H. Kumigashira, T. Yokoya, A. Chainani, T. Takahashi, H. Takeya, and K. Kadowaki, Phys. Rev. B **53**, R11 946 (1996).
¹⁴H.-D. Kim, O. Tjernberg, G. Chiaia, H. Kumigashira, T. Takahashi, L. Duó, O. Sakai, M. Kasaya, and I. Lindau, Phys. Rev. B **56**, 1620 (1997).
¹⁵L. Duo, Surf. Sci. Rep. **32**, 233 (1998).
¹⁶M.P. Seah and W.A. Dench, Surf. Interface Anal. **1**, 2 (1979).
¹⁷C.D. Wagner, L.E. Davis, and M. Riggs, Surf. Interface Anal. **2**, 53 (1980).
¹⁸Y. Saitoh, H. Kimura, Y. Suzuki, T. Nakatani, T. Matsushita, T. Muro, T. Miyahara, M. Fujisawa, K. Soda, S. Ueda, H. Harada, M. Kotsugi, A. Sekiyama, and S. Suga, Rev. Sci. Instrum. **71**, 3254 (2000).
¹⁹C. Laubschat, E. Weschke, C. Holtz, M. Domke, O. Strebel, and

- G. Kaindl, *Phys. Rev. Lett.* **65**, 1639 (1990).
- ²⁰A. Sekiyama, T. Iwasaki, K. Matsuda, Y. Saitoh, Y. Onuki, and S. Suga, *Nature (London)* **403**, 396 (2000).
- ²¹S.-H. Yang, S.-J. Oh, H.-D. Kim, R.-J. Jung, A. Sekiyama, T. Iwasaki, S. Suga, Y. Saitoh, E.-J. Cho, and J.-G. Park, *Phys. Rev. B* **61**, R13 329 (2000).
- ²²R.-J. Jung, H.-D. Kim, B.-H. Choi, S.-J. Oh, E.-J. Cho, T. Iwasaki, A. Sekiyama, S. Imada, S. Suga, and J.-G. Park, *J. Electron Spectrosc. Relat. Phenom.* **114–116**, 693 (2001).
- ²³R.-J. Jung, B.-H. Choi, J.-H. Kim, J.-G. Chung, S.-J. Oh, E.-J. Cho, T. Muro, A. Sekiyama, S. Imada, S. Suga, J.-G. Park, and Y. S. Kwon (unpublished).
- ²⁴B.-H. Choi, R.-J. Jung, H.-D. Kim, S.-J. Oh, E.-J. Cho, T. Iwasaki, Y. Saitoh, A. Sekiyama, S. Imada, S. Suga, J.-G. Park, and Y. S. Kwon (unpublished).
- ²⁵J.C. Fuggle, F.U. Hillebrecht, J.-M. Esteve, R.C. Karnatak, O. Gunnarsson, and K. Schonhammer, *Phys. Rev. B* **27**, 4637 (1983).
- ²⁶T. Jo, and A. Kotani, *Phys. Rev. B* **38**, 830 (1988).
- ²⁷L.C. Davis, *J. Appl. Phys.* **59**, R25 (1986).